Neural Network-Based Resilient Consensus Control of Nonlinear Multi-Agent Systems under Stochastic Disturbances and Cyber-Physical Attacks

Jun Du[1],Muhammad Zahid[2], Azmat Ullah Khan Niazi[2,*], Hanen Louati[3,*], Naveed Iqbal[4] and Mohammed M. A. Almazah[5]

[1] School of Finance and Mathematics, Huainan Normal University, Huainan, 232038, China

[2] Department of Mathematics and Statistics, The University of Lahore, Sargodha, 40100, Pakistan

[3] Mathematics Department, Faculty of Science, Northern Border University, Arar, 73222, Saudi Arabia

[4] Department of Mathematics, College of Science, University of Ha'il, Ha'il, 2440, Saudi Arabia

[5] Department of Mathematics, College of Sciences and Arts, King Khalid University, Muhyil, 61421, Saudi Arabia

INFORMATION

Keywords:
Stochastic disturbance
cyber-physical attacks
neural network
consensus control

DOI: 10.23967/j.rimni.2026.10.76520

Revista Internacional de Métodos Numéricos para Cálculo y Diseño en Ingeniería

Neural Network-Based Resilient Consensus Control of Nonlinear Multi-Agent Systems under Stochastic Disturbances and Cyber-Physical Attacks

Jun Du[1], **Muhammad Zahid**[2], **Azmat Ullah Khan Niazi**[2,*], **Hanen Louati**[3,*], **Naveed Iqbal**[4] and **Mohammed M. A. Almazah**[5]

[1]School of Finance and Mathematics, Huainan Normal University, Huainan, 232038, China

[2]Department of Mathematics and Statistics, The University of Lahore, Sargodha, 40100, Pakistan

[3]Mathematics Department, Faculty of Science, Northern Border University, Arar, 73222, Saudi Arabia

[4]Department of Mathematics, College of Science, University of Ha'il, Ha'il, 2440, Saudi Arabia

[5]Department of Mathematics, College of Sciences and Arts, King Khalid University, Muhyil, 61421, Saudi Arabia

ABSTRACT

For nonlinear multi-agent systems (MASs) vulnerable to stochastic disturbances and cyber-physical attacks on both sensors and actuators, this paper proposes an adaptive self-triggered consensus control framework based on neural networks. By using a decentralized leader-follower event-triggered strategy, the method avoids Zeno behavior and drastically reduces communication overhead by updating local state estimates only at designated triggering instants. An adaptive mechanism compensates for actuator attacks, and a neural network is integrated to approximate unknown nonlinear dynamics, thereby improving robustness against malicious attacks and uncertainties. To ensure stability, a lower bound on inter-event times is derived, and practical consensus is demonstrated using Lyapunov-Krasovskii analysis. Both homogeneous and heterogeneous MASs' numerical simulations confirm that the technique guarantees bounded state convergence and reduces the impact of attacks.

OPEN ACCESS

Received: 22/11/2025

Accepted: 24/12/2025

DOI
10.23967/j.rimni.2026.10.76520

Keywords:
Stochastic disturbance
cyber-physical attacks
neural network
consensus control

1 Introduction

With numerous applications in multi-agent formation, unmanned aerial vehicles [1], smart grids, and regular monitoring [2], consensus control is a crucial problem in cooperative control. Rather, it ensures that agents can collectively agree on a common position by interacting only with their local neighbors [3]. Despite this, in practice, multi-agent systems (MASs) often converge to a bounded region around the equilibrium point rather than a precise single state [4]. This is known as practical consensus [5], and is most often caused by unknown system dynamics, physical constraints, communication noise, or stochastic random effects [6]. Moreover, cyber-physical threats, such as cyber-physical attacks, can undermine the reliability of multi-agent systems (MASs) [7]. Enemy attacks can intentionally interfere with data or command signals, resulting in erroneous or distorted local data exchanges [8].

*Correspondence: Azmat Ullah Khan Niazi, Hanen Louati (azmatullah.khan@math.uol.edu.pk, hanen.louati@nbu.edu.sa).

Such attacks, when integrated with random communication noise, can severely undermine system performance and potentially destabilize the network [9]. To address these issues, some efforts have focused on developing distributed protocols and algorithms with more practical resilient [10], and robust consensus performance tailored to more realistic system assumptions and weaker constraints [11]. In recent years, considerable research has been conducted on the concept of event-triggered control, which aims to reduce energy consumption [12]. Significant progress has been documented in first-order, second-order, and even more general event-triggering frameworks for linear multi-agent systems (MASs) [13]. For MASs with first-order dynamics, for example, self-triggered consensus techniques have been put forth, where each agent updates its state by averaging the states of its neighbors [14]. In these situations, input updates and the timing of information exchange are controlled by event-triggered mechanisms [15]. Additionally, suggested a control update leader-follower control strategy for MASs under directed communication. The control signal was also based on neighboring states and was updated in a time-triggered way [16]. An adaptive event-triggered fault-tolerant control for linear MASs was also developed, where the control relied solely on local neighbor interactions and, as Zeno behavior was avoided, the system could run indefinitely without triggering a halt [17]. It is possible to design an adaptive event-triggered control algorithm by using online parameter estimation [18].

Considerable progress has also been made on event-triggered consensus control for nonlinear MASs. For instance, in [19], the collected-data problem of control for uncertain nonlinear systems was investigated, and a co-design method [20] was developed that simultaneously determines event triggers and feedback laws [21], a sliding mode based method was proposed to achieve desire equilibrium respecting time consensus in networked Lagrangian systems to guaranty semi-global ultimate boundedness and output tracking consensus [22]. The problem becomes more complicated in the presence of stochastic disturbances and cyber-physical attacks for the event-triggered mechanism [23]. Agents can be misled and consensus performance can be degraded because random communication noise may corrupt transmitted information, and adversaries can intentionally insert cyber-physical attacks into the trigger and state exchange channels [24]. Thus, resilient event-triggered control strategies are needed that cope with stochastic uncertainties and malicious data corruption to guarantee secure and robust cooperation in practical MASs [25].

When it comes to directed interaction topology, the problem of event-triggered control for nonlinear multi-agent systems (MASs) is still mostly unsolved, especially in the scenario of unknown agents' dynamic functions [26]. The authors of the reference address the fixed-time consensus problem of nonlinear multi-agent systems (MASs) with uncertainties in [27], using an event-triggered method that is limited to nonlinear dynamics with a known Lipschitz constant. The work in reference looked into the leader-following event-triggered consensus problem for Lipschitz nonlinear MASs and, in contrast to [28], did not require the prior knowledge of the Lipschitz constant [29]. There is no doubt that adaptive fuzzy controllers can deal with the nonlinear dynamics of systems with unknown parameters [30], few studies have examined fuzzy event-triggered consensus control, even though fuzzy systems and neural networks have influenced many different strategies [31], to the author's best knowledge, there are no studies on adaptive event-triggered consensus control for MASs using neural networks [32]. Adaptive fuzzy event-triggered control for a class of nonlinear multi-agent systems has been studied using backstepping techniques, while reach equilibrium adaptive leader-following control has been developed for multi-agent systems using back-stepping methods [33].

However, many practically relevant nonlinear systems, particularly when subjected to stochastic disturbances or cyber attacks, cannot be rigorously demonstrated to satisfy the Lipschitz condition or the strict-feedback form [34], random communications noise corrupts triggering signals, whereas cyber physical attacks would typically alter actual transmitted data among agents with the intent of malicious trimming of triggering instants and depletion of consensus performance [35]. These challenges indicate the need for adaptive, resilient, event-triggered strategies based on neural networks and robust approximation techniques to ensure reliable consensus of nonlinear MASs with unknown dynamics under stochastic uncertainties as well as under antagonistic attacks. The following is a summary of this work's primary contributions. To the best of the authors' knowledge, this is the first successful neural network-based adaptive control event-triggered consensus control methodology [36] for nonlinear MASs under sensor saturation. Both homogeneous and heterogeneous agent dynamics can benefit from the suggested method, which guarantees resilience to cyber-physical attacks and robustness against stochastic communication disruptions. Additionally, the self-triggered approach goes beyond traditional event-triggered control [37] by facilitating a distributed communication pattern that improves networked systems' security and energy efficiency. To effectively handle sensor nonlinearities under stochastic uncertainties and adversarial data manipulation, this work adopts and extends the convex hull procedure, which is typically used for actuator saturation, as opposed to the conventional sector condition method that is frequently used to address sensor saturation.

The main contribution of the paper is as follows:

- For a wide class of nonlinear multi-agent systems (MASs) that are simultaneously subject to stochastic disturbances, sensor saturation, and cyber-physical attacks on both sensors and actuators, a novel neural-network-based resilient self-triggered consensus framework is developed. The suggested framework greatly relaxes modeling assumptions by not requiring Lipschitz conditions, strict-feedback structures, or known system nonlinearities, in contrast to the majority of existing results.
- The consensus controller incorporates an adaptive neural network approximation mechanism to estimate malicious attack signals and unknown nonlinear dynamics online. In contrast to previous event-triggered consensus literature, the suggested NN-based compensation scheme ensures robustness against adversarial data manipulation and stochastic uncertainties, as well as bounded weight estimation errors.
- In order to effectively eliminate Zeno behavior and significantly reduce communication and computation burden, a distributed self-triggered communication strategy is proposed that determines triggering instants without continuous monitoring. The scheme is completely decentralized and scalable because the triggering rule only relies on locally accessible data.
- To demonstrate that the closed-loop MAS achieves practical consensus with an explicitly characterized ultimate bound even in the presence of stochastic disturbances and cyber-physical attacks, a rigorous Lyapunov–Krasovskii-based stochastic stability analysis is established. An analytical lower bound on inter-event times that is strictly positive is obtained.
- The proposed method's generality and applicability are demonstrated by handling both homogeneous and heterogeneous nonlinear MASs within a single control framework. In contrast, a lot of current methods are limited to homogeneous agent dynamics.
- Extensive simulation studies, including comparative analyses with baseline consensus techniques, confirm that the suggested method achieves reduced communication frequency, enhanced resilience to attacks, and faster convergence, underscoring its superiority in terms of security, efficiency, and robustness.

The Strategies Used

1. Section 1 introduces the consensus control problem of nonlinear multi-agent systems under stochastic disturbances, sensor saturation, and cyber physical attacks, and motivates the need for resilient control strategies.
2. In Section 2, the mathematical underpinnings are established, which include graph theory, a system model with disturbances or attacks, control input design, and the assumptions or lemmas required for the analysis.
3. The control strategy is developed in Section 3, stability proofs are given using Lyapunov theory, and it is demonstrated that the suggested scheme achieves secure, robust, and Zeno-free practical consensus.
4. In Section 4, validation of the theoretical results through simulations, showing that the proposed scheme ensures robust and efficient consensus in both homogeneous and heterogeneous multi-agent systems.
5. In Section 5, we sum up conclusions.

2 Preliminaries

2.1 Graph Theory

The directed graph $\mathcal{F} = (\mathcal{U}, \zeta)$ is used in this study to model the communication topology among agents. The sets of nodes and edges are represented by $\mathcal{U}$ and $\zeta \subseteq \mathcal{U} \times \mathcal{U}$. The corresponding adjacency matrix is represented as $\mathcal{B} = (b_{ij})$, where $b_{ii} = 0$ and $b_{ij} = 1$ if $(i, j) \in \zeta$, meaning that agent i can receive data from agent j; if not, $b_{ij} = 0$. These components are then used to define the Laplacian matrix $\mathcal{L}$ associated with the graph.

$$\mathcal{L}_{ij} = -b_{ij}, \quad i \neq j,$$

and

$$\mathcal{L}_{ii} = \sum_{j \neq i} b_{ij}.$$

The graph agent is indexed as $\{1, 2, \ldots, M\}$.

Assumption 1: *There is a spanning tree in the directed graph $\mathcal{F}$ that represents the communication mode.*

2.2 Problem Statement

The following equation controls each agent's dynamics:

$$\mathrm{d}s_i(t) = \left[\psi\big(s_i(t)\big) + u_i(t) + \hat{u}_i^a\right]\mathrm{d}t + h_i\big(s_i(t)\big)\,\mathrm{d}W_i(t), \qquad i = 1, \ldots, M. \tag{1}$$

The stochastic dynamics of the i-th agent in the multi-agent system is described by Eq. (1). $u_i(t)$ indicates the control input intended to accomplish the intended coordination goal, whereas $\psi(s_i(t))$ represents the agent's intrinsic nonlinear dynamics. The estimated compensation input that offsets adversarial influences, like cyber-physical attacks, is represented by the additional term $\hat{u}_i^a$. The term $h_i(s_i(t))\,\mathrm{d}W_i(t)$ represents the stochastic disturbance, where $h_i(s_i(t))$ is the diffusion coefficient and $\mathrm{d}W_i(t)$ is the increment of a standard Wiener process. A thorough depiction of the system under uncertainty and possible hostile attacks is thus provided by the state evolution of each agent, which is driven by its intrinsic nonlinear dynamics, the control and compensation inputs that are designed, and random environmental fluctuations.

The equation of control input is:

$$u_i(t) = -K_i^k(t)e_i(t) + v_i(t) - \hat{u}_i^a(t) - \sigma_i e_i, \qquad i = 1, \ldots, M \tag{2}$$

The feedback term $-K_i^k(t)e_i(t)$ ensures practical consensus among the agents and $v_i(t)$ is a function of $\check{s}_i(t)$. The component $\hat{u}_i^a(t)$ enhances resilience against adversarial inputs by representing the estimated impact of possible attacks or disturbances. By adding more robustness to the system, the additional damping term $-\sigma_i e_i$ is specifically introduced to lessen the impact of stochastic disturbances. This term aids in maintaining stable formation tracking by lowering the variance of the agent states in noisy environments. All things considered, the suggested controller combines stochastic robustness, attack resilience, nonlinear compensation, and consensus enforcement into a single framework.

$e_i(t) = \sum_{j=1}^{N} b_{ij}\left(\check{s}_i(t) - \check{s}_j^i(t)\right)$, where $\check{s}_i(t) = s_i(\tau_k^i)$, $\check{s}_j^i(t) = s_j(\tau_k^i)$, $\tau_k^i \le t < \tau_{k+1}^i$, and k is a positive integer.

Note that $\tau_i^1, \tau_i^2, \tau_i^3, \ldots$ is a sequence of monotonically increasing time instants with $\tau_0^i = 0$, such that $\tau_{k+1}^i > \tau_k^i$, and $\tau_k^i \to \infty$ while $k \to \infty$. These represent the times when the event-triggered condition is breached.

Remark 1: *Four major parts make up the controller in Eq. (2). The feedback regulation mechanism that pushes the agents toward practical consensus while managing feedback is provided by the first term, $-K_i^k(t)\,(e_i(t))$. Neural networks can be used to design the second term $v_i(t)$ which can be used in Assumption 2, which compensates for the agent's unknown nonlinear dynamics. By deducting an online estimate of the adversarial input, the third term, $-\hat{u}_i^a(t)$, specifically addresses the impact of cyber-physical attacks. Lastly, the damping term $-\sigma_i e_i(t)$ improves robustness in noisy environments by reducing the impact of stochastic disturbances.*

Assumption 2: $ds_i(t) = \left(\psi(s_i(t)) + v_i^d(t) + u_i^a(t)\right)\mathrm{d}t + h_i(s_i(t))\,\mathrm{d}W_i(t)$, *describes the system dynamics in the presence of stochastic disturbances and cyber physical attacks. Where $h_i(s_i), \mathrm{d}W_i(t)$ models the stochastic disturbance, $u_i^a(t)$ represents the cyber physical attack signal, and $v_i^d(t)$ indicates the ideal control input. It is assumed that even in the presence of stochastic disturbances and attacks, the system is still controllable and input-to-state linearizable.*

Remark 2: *The existence of an optimal control input $v_i^d(t)$ that offsets the unknown nonlinear dynamics $\psi(s_i(t))$ is guaranteed by Assumption 2. Consequently, the closed-loop system*

$$ds_i(t) = \left(\psi(s_i(t))\,\mathrm{d}t + v_i^d(t) + u_i^a(t)\right)\mathrm{d}t + h_i(s_i(t))\,\mathrm{d}W_i(t) \tag{3}$$

remains stable despite stochastic disturbances $h_i(s_i)\mathrm{d}W_i(t)$ and cyber physical attacks $u_i^a(t)$. The nonlinear dynamics in this context can be expressed in a linear input-to-state form as follows: $ds_i(t) = \left(As_i(t) + u_i^a(t)\right)dt + h_i(s_i(t))\,W_i(t)$, Hurwitz matrix [38] is represented by A. The same matrix may be applied to all agents, regardless of whether their intrinsic dynamics differ, because A is freely assignable. This characteristic ensures that the suggested control framework is robust against adversarial inputs and stochastic uncertainties, and that it is still applicable to both homogeneous and heterogeneous multi-agent systems.

Remark 3: *[39] The event-triggered consensus control of nonlinear MASs requires that the system's nonlinear dynamics meet the Lipschitz condition or more stringent structural inequalities. This paper, on the other hand, significantly loosens the modeling assumptions by requiring the feedback linearization [40]. The suggested method enriches the study of event-triggered consensus control for nonlinear MASs* *by imposing no structural constraints, in contrast to fuzzy-based approaches [41] that require lower triangular structures.*

The $v_i^d(t)$ cannot be directly designed in Assumption 2 since the $\psi(s_i(t))$ is unknown and further corrupted by both stochastic disturbances and cyber physical attacks. A neural network (NN) is used as an adaptive approach to overcome this difficulty. The NN builds computational models with nodes connected by weighted edges and each node having an activation function, drawing inspiration from the information-processing power of human neurons. Sigmoid, ReLU, and hyperbolic tangent are examples of common activation functions; the latter is employed in this investigation. The NN's memory is represented by the weighted interconnections, and the weights, activation functions, and network connectivity all affect the output. This feature enables the NN to approximate unknown nonlinear dynamics even when adversarial signals and stochastic fluctuations are present. Therefore, the equation of $v_i^d(t)$ is as follows:

$$v_i^d(t) = M_{vi^d}^T \, q_v(\bar{s}_i(t)) + \epsilon_{vi}(s_i(t)), \tag{4}$$

$M_{vi^d} \in \mathbb{R}^{l\times m}$ represents the ideal weight matrix that relate to $v_i^d(t)$, $q_v(\bar{s}_i(t)) \in \mathbb{R}^l$ is the activation function vector, $\bar{s}_i = H_v^T s_i(t)$ and $H_v \in \mathbb{R}^{m\times l}$ is the input-layer weight matrix, and $\epsilon_{vi}^d(s_i(t)) \in \mathbb{R}^m$ is the NN reconstruction error. Thus, the NN approximation ensures the resilience of the consensus protocol for both homogeneous and heterogeneous multi-agent systems by offering a strong mechanism to estimate the optimal control input under stochastic disturbances and malevolent attacks.

Assumption 3: *Even when stochastic disturbances and cyber physical attacks are present, the activation function $q_v(\bar{o})$ of the NN is Lipschitz continuous on a bounded set $\Omega_o \subset \mathbb{R}^m$. In particular, for each $o_1, o_2 \in \Omega_o$, there exists a constant $L_{q_v} > 0$ such that $\|q_v(\bar{o}_1) - q_v(\bar{o}_2)\| \leq L_{q_v} \|o_1 - o_2\|$, where $\bar{o} = H_v^T o$, $\bar{o}_1 = H_v^T o_1$, and $\bar{o}_2 = H_v^T o_2$, where H_v is the NN input-layer weight matrix. The NN approximation is guaranteed to stay stable in the face of adversarial data manipulation and stochastic perturbations thanks to the bounded Lipschitz continuity.*

Assumption 4: *Even in the face of cyber physical attacks and stochastic disturbances, M_v is the target weight matrix, $q_v(\cdot)$ is the function of activation, and $\epsilon_v(\cdot)$ is the mistake of the neural network, which is bounded in upper and has in compact form. In particular,*

$$\|M_v\| \leq M_{v,\max}, \quad \|q_v(\cdot)\| \leq q_{v,\max}, \quad \|\epsilon_v(\cdot)\| \leq \epsilon_{v,\max},$$

AS $M_{v,\max}$, $q_{v,\max}$, and $\epsilon_{v,\max}$, these constant have positive value. The robustness of the consensus protocol under adversarial data manipulation and stochastic perturbations depends on these bounds, which ensure that the NN approximation stays uniformly bounded.

Definition 1: *[15] The Eq. (1) reach consensus if ε is positive, and control input Eq. (2) and time $T \geq 0$ depending on ε and initial conditions $s_i(t_0)$ for all $i = 1, 2, \ldots$ such that $\|s_i(t) - s_j(t)\| \leq \varepsilon, \quad \forall t \geq t_0 + T, \quad \forall i, j = 1, 2, \ldots$ Let $\mathbb{A}$ denote the set of all $m \times m$ diagonal matrices whose diagonal entries are either 0 or 1. The set $\mathbb{A}$ contains exactly 2^m such matrices, denoted as A_i, where $i = 1, 2, \ldots, 2^m$.*

Lemma 1: *[37] Let $u, v \in \mathbb{R}^m$ with $u = [u_1, u_2, \ldots, u_m]^T$ and $v = [v_1, v_2, \ldots, v_m]^T$. Suppose that $|v_i| \leq 1$ holds for all $i \in \{1, 2, \ldots, m\}$. Then, the following relation holds:*

$$u \in \text{co}\left\{A_i u + (I - A_i)v : i \in \{1, 2, \ldots, 2^m\}\right\}, \tag{5}$$

in which $A_i \in \mathbb{A}$, and $\text{co}\{\cdot\}$ denotes the minimal convex set. The estimation of error is $\tilde{s}_i(t) = s_i(t) - \check{s}_i(t)$. The following lemma will be useful in the subsequent analysis.

Lemma 2: *[33] Suppose that $g(s_i(t)) : \Omega_s \to \mathbb{R}^m$ represents a continuous function defined in a bounded set, where $s_i(t) \in \Omega_s \subset \mathbb{R}^m$. Whereas, using constant weights and an event-triggered activation function, a single-layer neural network (NN) can approximate $g(s_i(t))$ so that*

$$g(s_i(t)) = M^T q\big(\check{s}_i(t)\big) + \varepsilon\big(\check{s}_i(t), \tilde{s}_i(t)\big), \tag{6}$$

where $M \in \mathbb{R}^{l\times m}$ denotes the weight matrix of the target neural network, $q(\check{s}_i(t)) \in \mathbb{R}^l$ represents the bounded event-driven activation function, and $\varepsilon(\check{s}_i(t), \tilde{s}_i)$ is the approximation error.

According to Lemma 2, the control input

$$v_i(t) = \hat{M}_{v_i}^T(t)\, q_v\big(\bar{\check{s}}_i(t)\big), \quad \tau_k^i \le t < \tau_{k+1}^i, \tag{7}$$

where $\hat{M}_{v_i}(t) \in \mathbb{R}^{l\times m}$ denotes the estimated NN weight matrix, initialized arbitrarily at $\hat{M}_{v_i}(0)$, and $q_v(\bar{\check{s}}_i(t)) \in \mathbb{R}^l$ is the event-triggered activation function. Here, the NN input is defined as $\bar{\check{s}}_i(t) = H_v^T \check{s}_i(t)$. For notational convenience, we let $s_i = s_i(t)$, $s_i^+ = s_i(t^+)$, $\hat{M}_{v_i} = \hat{M}_{v_i}(t)$, $\hat{M}_{v_i}^+ = \hat{M}_{v_i}(t^+)$, and $K_k^i = K_k^i(t)$ in the following content. During the inter-event intervals $\tau_k^i \le t < \tau_{k+1}^i$, the estimated NN weights remain constant:

$$d\hat{M}_{vi}(t) = 0 \cdot dt + h_i(s_i(t)\, dW_i(t), \quad \tau_i^k \le t < \tau_i^{k+1} \tag{8}$$

At each event-triggered instant $t = \tau_k^i$, the weight update law is defined as

$$\hat{M}_{vi}^+ = \hat{M}_{vi} - \frac{\alpha_v}{c + \|\tilde{s}_i\|^2}\, q_v(\bar{s}_i)\, \big(\tilde{s}_i + \eta_i + a_i^s\big)^T L - \kappa \hat{M}_{vi} + h_i(s_i(t))\, dW_i(t), \tag{9}$$

where α_v, c, and κ are positive design parameters. Let $\alpha_v > 0$ be the neural network, which can be chosen randomly. The constant $c \ge \frac{1}{4}$, the matrix $L \in \mathbb{R}^{m\times m}$ can also be selected arbitrarily, and $\kappa \in \left(0, \dfrac{1}{2}\right)$ is a positive constant. Next, the error in weight estimation is defined as $\tilde{M}_{vi} = M_v - \hat{M}_{vi}$, where η_i represents the stochastic disturbance. a_i^s is the injected false data signal, $h_i(s_i(t))$, $dW_i(t)$ model stochastic diffusion in the weight update. Whose dynamics are given by

$$\begin{cases} d\tilde{M}_{vi}(t) = -\, h_i(s_i(t))\, dW_i(t), & \tau_i^k \le t < \tau_i^{k+1}, \\ \tilde{M}_{vi}^+ = \tilde{M}_{vi} + \alpha_v\, \chi_i\, q_v(\bar{x}_i)\, \big(\tilde{s}_i + \eta_i + a_i^s\big)^\top L + \kappa\, \hat{W}_{vi}, & t = \tau_i^k, \end{cases} \tag{10}$$

where $\chi_i = \dfrac{1}{c + \|\tilde{s}_i\|^2}$. The closed-loop system dynamics during the inter-event interval $\tau_k^i \le t < \tau_{k+1}^i$ are expressed as

$$ds_i = \Big(\psi(s_i) + \hat{M}_{vi}^\top q_v(\check{s}_i) - K_i^k(e_i)\Big)\, dt + h_i(s_i(t))\, dW_i(t), \quad \tau_i^k \le t < \tau_i^{k+1}. \tag{11}$$

The desired control term v_i^d, we get

$$ds_i = \big(\psi(s_i) + \hat{M}_{v_i}^\top q_v\big(\bar{\check{s}}_i\big) + v_i^d - v_i^d - K_k^i e_i\big)dt + h_i(s_i(t))\, \mathrm{d}W_i(t), \quad \tau_k^i \le t < \tau_{k+1}^i, \tag{12}$$

therefore

$$ds_i = \big(As_i + \hat{W}_v^T q_v(\bar{s}_i) - W_v^T q_v(\bar{s}_i) - \varepsilon_v(s_i) - K_i^k(e_i)\big)dt + h_i(s_i(t))\, \mathrm{d}W_i(t), \qquad \tau_k^i \le t < \tau_{k+1}^i \tag{13}$$

Using the relation $M_v = \tilde{M}_{vi} + \hat{M}_{vi}$, the overall closed-loop dynamics, the state behavior at event-triggered moments, and the error dynamics of the weight estimates are described for $\tau_k^i \le t < \tau_{k+1}^i$.

$$\begin{cases} ds_i &= \Big[As_i - \big(\tilde{M}_{vi}^\top q_v(\bar{s}_i) + \varepsilon_v(s_i)\big) + \hat{M}_{vi}^\top q_v(\bar{\check{s}}_i) - \hat{M}_{vi}^\top q_v(\bar{s}_i) - K_i^k\big(e_i\big) + (u_i^a - \hat{u}_i^a)\Big]dt \\ & +h_i(s_i(t))\,dW_i(t), \\ d\check{s}_i &= 0, \qquad \text{(zero-order hold between events)} \\ d\hat{M}_{vi} &= 0, \qquad \text{(weight frozen between events)} \end{cases} \tag{14}$$

At the event-triggered instant $t = \tau_k^i$, the system undergoes discrete updates given by:

$$\begin{cases} s_i^+ &= s_i, \\ \check{s}_i^+ &= s_i \ + \ \eta_i \ + \ a_i^s, \\ \tilde{M}_{vi}^+ &= \tilde{M}_{vi} \ + \ \alpha_v \chi_i \, q_v\big(\bar{s}_i\big)\,\big(\tilde{s}_i\big)^\top L \ + \ \kappa \hat{M}_{vi} \end{cases} \tag{15}$$

The corresponding jump dynamics are as follows

$$\begin{cases} \Delta s_i &= s_i^+ - s_i = 0, \\ \Delta \check{s}_i &= \check{s}_i^+ - \check{s}_i = \tilde{s}_i = \tilde{s}_i + \eta_i + a_i^s, \\ \Delta \tilde{M}_{vi} &= \tilde{M}_{vi}^+ - \tilde{M}_{vi} = \alpha_v \, \chi_i \, q_v\big(\bar{s}_i\big)\,\big(\tilde{s}_i\big)^\top L \ + \ \kappa \, \hat{M}_{vi} \end{cases} \tag{16}$$

The event-triggering condition is defined as

$$\tau_i^{k+1} = \inf_{t > \tau_i^k} \left\{ t \;\middle|\; \begin{array}{ll} & \|\tilde{s}_i\| = \dfrac{1}{L_q \, \|\hat{M}_{vi}\|} \left(\dfrac{q_{\min}\Gamma}{4\|P\|} \|s_i\| - K_i^k \, \|e_i\| \, A_{\max} + \dfrac{\varsigma}{\|P\|} + \Delta_i \right), \\ \text{and} & \|s_i\| \ge B_x^{\max} \end{array} \right\}, \tag{17}$$

where $P, Q \in \mathbb{R}^{m\times m}$ are symmetric positive definite matrices satisfying $A^T P + PA = -Q$, $q_{\min}$ is the minimum eigenvalue of Q, $0 < \Gamma < 1$, and $A_{\max} = \max(\|A_l + (I_n - A_l)H\|)$, with $H \in \mathbb{R}^{m\times m}$, $\varsigma > 0$, and $B_s^{\max}$ is the expected bound of $\|s_i\|$. The step function K_k^i is defined as:

$$\begin{cases} \dot{K}_k^i &= 0, \qquad \tau_i^k \le t < \tau_i^{k+1}, \\ K_k^{i+} &\le \min\left\{ K_i^{\max}, \ \dfrac{q_{\min}\,\Gamma\,\|s_i\|}{4A_{\max}\,\|P\|\,\|e_i\| + \Delta_i + \varepsilon)} \right\}, \qquad t = \tau_i^{k+1}, \\ K_k^i &\ge 0 \end{cases} \tag{18}$$

The region for i is defined as:

$$M(H)_{[i]} := \{s_i : \left(\left\| H \sum_{j=1}^{N} b_{ij}(\check{s}_i - \check{s}_j) \right\|_\infty \le 1 \right\} \tag{19}$$

And the overall unsaturated region for the network is:

$$M(H) := \left\{s \in \mathbb{R}^{mM} : \|(I_M \otimes H)(L \otimes I_m)\, s\|_\infty \leq 1\right\} \tag{20}$$

where $s = [s_1^T, \dots, s_N^T]^T \in \mathbb{R}^{mM}$, L is the Laplacian matrix of the communication graph, and $\otimes$ denotes the Kronecker product.

Definition 2: *The value of $\Gamma > 0$ and a positive definite matrix $P > 0$ define the Lyapunov function candidate as $\tilde{V}(t) = s_i^T P s_i$. The symmetric polyhedron is then denoted by $\mathcal{F}(P, \Gamma) = \left\{s : s^T(I_M \otimes P)s \leq \Gamma\right\}$. This set $\mathcal{F}(P, \Gamma)$ is called a strictly invariant set of system of Eq. (1) if the following conditions hold: $d\tilde{V}(t) < 0$, for $\tau_k^i \leq t < \tau_{k+1}^i$, and $\Delta\tilde{V}(\tau_k^i) < 0$, for all $s \in \psi(P, \Gamma) \setminus \mathcal{S}(B_{\max}^s)$, where $\mathcal{S}(B_{\max}^s) := \left\{s : \|s_i\| < B_{\max}^s\right\}$.*

Lemma 3: If there is a positive definite, continuously differentiable, and radially unbounded function $dV(s)$ defined on $\mathbb{R}^m$ such that $dV(s)$ is negative definite in $\mathbb{R}^m$, then the foundation is universally ultimately balanced.

3 Main Results

This section will provide a self-triggered system that avoids Zeno behavior for a family of nonlinear MASs with stochastic disturbance and cyber-physical attack based on a neural network.

Theorem 1: *Suppose that the nonlinear MAS Eq. (1) with control inputs Eqs. (2) and (7), the event-trigger condition 17, and the NN update rules Eqs. (8) and (9). Assume that $F(P, \Gamma) \subset M(H)$ and Assumptions 1–4 hold. The MAS can reach practical agreement whenever the inter-event interval has a strictly positive lower bound, represented by $\delta\tau_k^i = \tau_{k+1}^i - \tau_k^i > 0$, for $k = 0, 1, \dots, i = 1, 2, \dots,$ and the system invariant region $\psi(p, \Gamma)$.*

Proof: The proof has two sequential steps. First, we show that the norm $\|s_i\|$ is an auxiliary variable bound. In the second step, we demonstrate that this variable is itself limited and can be made small by appropriately tuning the control constants.

Step 1: The Lyapunov function:

$$V_{s_i} = s_i^T P s_i. \tag{21}$$

For the time interval $\tau_k^i \leq t < \tau_{k+1}^i$, the time derivative of V_{s_i} is given by

$$\begin{aligned} dV_{s_i} = \Big[&- s_i^\top Q s_i - 2\left(\tilde{M}_{vi}^\top q_v(\bar{s}_i) + \varepsilon_v(s_i)\right)^\top P s_i \\ &+ 2\left(\hat{M}_{vi}^\top q_v(\bar{\breve{s}}_i) - \hat{M}_{vi}^\top q_v(\bar{s}_i)\right)^\top P s_i \\ &- 2K_i^k\,(e_i)^\top P s_i + 2\left(u^a - \hat{u}^a\right)^\top P s_i \Big] dt \\ &+ 2\, s_i^\top P\, h_i(s_i(t))\, dW_i(t) \end{aligned} \tag{22}$$

Using Lemma 1, the Frobenius norm, and the Cauchy–Schwarz inequality, we estimate the time derivative of the Lyapunov function V_{s_i} as follows:

$$\begin{aligned} dV_{s_i} \leq \Big[&- \lambda_{\min}(Q)\,\|s_i\|^2 + 2\|\tilde{M}_{vi}\|\,\|q_v(\bar{s}_i)\|\,\|Ps_i\| + 2\|\varepsilon_v(s_i)\|\,\|Ps_i\| \\ &+ 2\left\| \hat{M}_{vi}^{\top} q_v(\breve{\bar{s}}_i) - \hat{M}_{vi}^{\top} q_v(\bar{s}_i) \right\| \|Ps_i\| \\ &- 2K_i^k\,(e_i)^{\top} Ps_i + 2\left(u^a - \hat{u}^a\right)^{\top} Ps_i \Big]\,dt \\ &+ 2\,s_i^{\top} P\,h_i(s_i(t))\,dW_i(t) \end{aligned} \tag{23}$$

Applying the Lipschitz continuity Assumption 3 and Young's inequality Eq. (23) to handle cross terms, we obtain:

$$\begin{aligned} dV_{s_i} \;\leq\; \Big[&-\; q_{\min}\,\|s_i\|^2 + \frac{q_{\min}}{2}\,\|s_i\|^2 + \frac{2}{q_{\min}}\|P\|^2\big(\,\|\tilde{M}_{vi}\|\,q_{v,\max} + \varepsilon_{v,\max}\big)^2 \\ &+\; 2L_{q_v}\,\|\hat{M}_{vi}\|\,\|P\|\,\|s_i\|\,\|\tilde{s}_i\| +\; 2K_i^k\,A_{\max}\,\|e_i\|\,\|P\|\,\|s_i\| \\ &+\; 2\,\|u^a - \hat{u}^a\|\,\|P\|\,\|s_i\| + \Big]\,dt \;+\; 2\,s_i^{\top} P\,h_i(s_i(t))\,dW_i(t). \end{aligned} \tag{24}$$

Using event-triggering condition (17), we derive the following

$$\begin{aligned} dV_{s_i} \leq \Big[&- \tfrac{c_1}{2}\|s_i\|^2 + c_2\|s_i\|\|\tilde{M}_{vi}\| + c_4\|s_i\|\left\|\hat{M}_{vi}^{\top} q_v(\breve{\bar{s}}_i) - \hat{M}_{vi}^{\top} q_v(\bar{s}_i)\right\| \\ &- 2K_i^k\,(e_i)^{\top} Ps_i + 2\,(u^a - \hat{u}^a)^{\top} Ps_i + \tfrac{c_3^2}{2c_1}\|\varepsilon_v(s_i)\|^2 \Big]\,dt \\ &+ 2\,s_i^{\top} P\,h_i(s_i(t))\,dW_i(t). \end{aligned} \tag{25}$$

From inequality Eq. (25), it follows that $\dot{V}_{s_i} < 0$ whenever

$$\|s_i\| > \left(\frac{8}{q_{\min}^2(1-\Gamma)} \|P\|^2(\|\tilde{M}_{v_i}\|q_{v,\max} + \varepsilon_{v,\max})^2 + \frac{16}{q_{\min}^2(1-\Gamma)^2}\varsigma^2 \right)^{1/2} = B_1^{x_i}.$$

At the triggering instant $t = \tau_k^i$, the jump in the Lyapunov function is:

$$\Delta V_{s_i} = s_i^{+T} P s_i^{+} - s_i^T P s_i = 2 s_i^T P\,\Delta s_i \;+\; \Delta s_i^T P\,\Delta s_i \tag{26}$$

From Eq. (15), we know that

$$\Delta V_{s_i} = 2 s_i^{\top} P\big(\eta_i + a_i^s\big) + \big(\eta_i + a_i^s\big)^{\top} P\big(\eta_i + a_i^s\big). \tag{27}$$

By Eqs. (25) and (27), we came to the conclusion that $s_i(t)$ ultimately converges to the set. $\{s_i \,:\, \|s_i\| \,\leq\, B_1^{s_i}\}$. However, since $B_1^{s_i}$ depends on the weight estimation error $\tilde{M}_{v_i}$, we now analyze its boundedness.

Step 2: Consider the Lyapunov function for the NN weight estimation error:

$$V_{\tilde{M}v_i} = \mathrm{vec}(\tilde{M}_{v_i})^T \mathrm{vec}(\tilde{M}_{v_i}) = \mathrm{tr}(\tilde{M}_{v_i}^T \tilde{M}_{v_i}). \tag{28}$$

For $\tau_k^i \leq t < \tau_{k+1}^i$, using (14), we have:

$$d\tilde{M}_{vi}(t) = -\,h_i(s_i(t))\,dW_i(t), \qquad \tau_i^k \leq t < \tau_i^{k+1}. \tag{29}$$

At the event-triggering instant $t = \tau_k^i$, the jump in $V_{\tilde{M}_{v_i}}$ becomes:

$$\begin{aligned}\Delta V_{\tilde{M}_{vi}} &= \mathrm{tr}\{(\tilde{M}_{vi}^{+})^{\top}\tilde{M}_{vi}^{+}\} - \mathrm{tr}\{\tilde{M}_{vi}^{\top}\tilde{M}_{vi}\} \\ &= 2\alpha_v\chi_i\,\mathrm{tr}\Big\{\tilde{M}_{vi}^{\top}q_v(\bar{s}_i)\big(\tilde{s}_i+\eta_i+a_i\big)^{\top}L\Big\} + 2\kappa\,\mathrm{tr}\{\tilde{M}_{vi}^{\top}\hat{M}_{vi}\} \\ &\quad + \alpha_v^2\chi_i^2\,\mathrm{tr}\Big\{\big(q_v(\bar{s}_i)\big(\tilde{s}_i+\eta_i+a_i^s\big)^{\top}L\big)^{\top}\big(q_v(\bar{x}_i)\big(\tilde{x}_i+\eta_i+a_i^s\big)^{\top}L\big)\Big\} \\ &\quad + 2\alpha_v\chi_i\kappa\,\mathrm{tr}\Big\{\big(q_v(\bar{s}_i)\big(\tilde{s}_i+\eta_i+a_i^s\big)^{\top}L\big)^{\top}\hat{M}_{vi}\Big\} + \kappa^2\,\mathrm{tr}\{\hat{M}_{vi}^{\top}\hat{M}_{vi}\}.\end{aligned} \tag{30}$$

From Eq. (15)

$$\begin{aligned}\Delta V_{\tilde{M}_{vi}} &= 2\alpha_v\chi_i\,\mathrm{tr}\Big\{\tilde{M}_{vi}^{\top}q_v(\bar{s}_i)\big(\tilde{s}_i+\eta_i+a_i^s\big)^{\top}L\Big\} + 2\kappa\,\mathrm{tr}\{\tilde{M}_{vi}^{\top}(M_v-\tilde{M}_{vi})\} \\ &\quad + \alpha_v^2\chi_i^2\,\mathrm{tr}\Big\{\big(q_v(\bar{s}_i)\big(\tilde{s}_i+\eta_i+a_{si}\big)^{\top}L\big)^{\top}\big(q_v(\bar{s}_i)\big(\tilde{s}_i+\eta_i+a_i^s\big)^{\top}L\big)\Big\} \\ &\quad + 2\alpha_v\chi_i\kappa\,\mathrm{tr}\Big\{\big(q_v(\bar{s}_i)\big(\tilde{s}_i+\eta_i+a_i^s\big)^{\top}L\big)^{\top}(M_v-\tilde{M}_{vi})\Big\} + \kappa^2\,\mathrm{tr}\{(M_v-\tilde{M}_{vi})^{\top}(M_v-\tilde{M}_{vi})\}.\end{aligned} \tag{31}$$

By replacing $\hat{M}_{vi} = M_v - \tilde{M}_{vi}$, the derivative of the Lyapunov function becomes:

$$\begin{aligned}\Delta V_{\tilde{M}_{vi}} &= 2\alpha_v\chi_i\,\mathrm{tr}\Big(\tilde{M}_{vi}^{\top}q_v(\bar{s}_i)\,(\tilde{s}_i+\eta_i+a_i^s)^{\top}L\Big) \\ &\quad + 2\kappa\,\mathrm{tr}\big(\tilde{M}_{vi}^{\top}\hat{M}_{vi}\big) \\ &\quad + \alpha_v^2\chi_i^2\,\mathrm{tr}\Big(\big[q_v(\bar{s}_i)\,(\tilde{s}_i+\eta_i+a_i^s)^{\top}L\big]^{\top}\big[q_v(\bar{s}_i)\,(\tilde{s}_i+\eta_i+a_i^s)^{\top}L\big]\Big) \\ &\quad + 2\alpha_v\chi_i\kappa\,\mathrm{tr}\Big(\big[q_v(\bar{s}_i)\,(\tilde{s}_i+\eta_i+a_i^s)^{\top}L\big]^{\top}\hat{M}_{vi}\Big) \\ &\quad + \kappa^2\,\mathrm{tr}\big(\hat{M}_{vi}^{\top}\hat{M}_{vi}\big).\end{aligned} \tag{32}$$

From Assumption 4 and applying the Cauchy-Schwarz inequality, we obtain the following upper bound:

$$\begin{aligned}\Delta V_{\tilde{M}_{vi}} &\le 2\alpha_v q_{v,\max}\chi_i\,\|\tilde{M}_{vi}\|\,\|L\|\,\|z_i\| + 2\kappa\,\|\tilde{M}_{vi}\|\,\|M_v\| - 2\kappa\,\|\tilde{M}_{vi}\|^2 \\ &\quad + \alpha_v^2\chi_i^2 q_{v,\max}^2\,\|L\|^2\,\|z_i\|^2 + 2\alpha_v\chi_i\kappa q_{v,\max}\,\|L\|\,\|z_i\|\,\|M_v\| \\ &\quad + 2\alpha_v\chi_i\kappa q_{v,\max}\,\|L\|\,\|z_i\|\,\|\tilde{M}_{vi}\| + 2\kappa^2\,\|\tilde{M}_{vi}\|^2 + 2\kappa^2\|M_v\|^2.\end{aligned} \tag{33}$$

Considering that $0 < \chi_i\|\tilde{s}_i\| \le 1$ with $c \ge 0.25$, and using Young's inequality on the 2nd term, the derivative of the Lyapunov function satisfies the following

$$\begin{aligned}\Delta V_{\tilde{M}_{vi}} &\le 2\alpha_v q_{v,\max}\chi_i\,\|\tilde{M}_{vi}\|\,\|L\|\,\|z_i\| + 2\kappa\,\|\tilde{M}_{vi}\|\,\|M_v\| - 2\kappa\,\|\tilde{M}_{vi}\|^2 \\ &\quad + \alpha_v^2\chi_i^2 q_{v,\max}^2\|L\|^2\|z_i\|^2 + 2\alpha_v\chi_i\kappa q_{v,\max}\|L\|\,\|z_i\|\,\|M_v\| \\ &\quad + 2\alpha_v\chi_i\kappa q_{v,\max}\|L\|\,\|z_i\|\,\|\tilde{M}_{vi}\| + 2\kappa^2\|\tilde{M}_{vi}\|^2 + 2\kappa^2\|M_v\|^2\end{aligned} \tag{34}$$

where

$$B^{M_v} = 2\,\alpha_v\, q_{v,\max}\,\kappa\,\|L\|\, M_{v,\max} \;+\; (\kappa + 2\kappa^2)\, M_{v,\max}^2 \;+\; \alpha_v^2 q_{v,\max}^2\,\|L\|^2. \tag{35}$$

Define constants:

$$a_1 = \kappa - 2\kappa^2 > 0 \quad \text{for} \quad 0 < \kappa < \frac{1}{2}, \qquad a_2 = 2\alpha_v q_{v,\max}(1+\kappa)\|L\|.$$

Then, inequality Eq. (34) becomes:

$$\Delta V_{\tilde{M}_{vi}} \;\leq\; -\,a_1\,\|\tilde{M}_{vi}\|^2 \;+\; a_2\,\|\tilde{M}_{vi}\| \;+\; B_{M_v} \tag{36}$$

By completing the square, we further obtain:

$$\Delta V_{\tilde{M}_{vi}} \leq -\frac{a_1}{2}\|\tilde{M}_{vi}\|^2 - \left(\sqrt{\frac{a_1}{2}}\|\tilde{M}_{vi}\| - \frac{a_2}{\sqrt{2a_1}}\right)^2 + B_1^{M_v}, \tag{37}$$

where

$$B_1^{M_v} = \frac{a_2^2}{2a_1} + B^{M_v}.$$

Thus, the Lyapunov function derivative is ultimately upper bounded by:

$$\Delta V_{\tilde{M}_{vi}} \leq -\frac{a_1}{2}\|\tilde{M}_{vi}\|^2 + B_1^{M_v}. \tag{38}$$

Consequently, from Eq. (38), $\Delta V_{\tilde{M}_{vi}} < 0$ until $\|\tilde{M}_{vi}\| > \sqrt{\frac{2B^1_{M_v}}{a_1}} = B^1_{\tilde{M}_v}$. By using of Lyapunov theorem in Lemma 3, the constant $\overline{T}$ such that the NN weight approximation error is completely bounded [42] for all $t > T$ at triggered time instants or for all $\tau_i^k > \overline{T}$, where T is a function of $\overline{T}$. This show that the system states s_i, $i = 1, \ldots, M$, From Eqs. (29) and (38) error in weight estimation is completely bounded. Specifically, the bound $B_1^{s_i}$ for each state s_i will approach to $B^s_{\max} = \frac{2}{q_{\min}\sqrt{1-\Gamma}}\|P\|\left(B_1^{\tilde{M}_v} q_{v,\max} + \varepsilon_{v,\max}\right)$, where Γ, α_v, κ, L, $q_{v,\max}$, and $\varepsilon_{v,\max}$ are design-tunable parameters. Therefore, for any desired bound $B^s_{\max}$, there exist a suitable control input 2 and a time $T \geq 0$ (dependent on $B^s_{\max}$ and the initial position $s_i(t_0)$) such that $\|s_i(t)\| \leq B^s_{\max} + \varepsilon_0, \quad t \geq T, \quad i = 1, \ldots, M$, where ε_0 is an arbitrarily small positive constant. Consequently, for any $\varepsilon > 0$, there exists a control law in Eq. (2) and a time $T_0 \geq 0$ (depending on ε and initial states $s_i(t_0)$) such that $\|s_i(t) - s_j(t)\| \leq \varepsilon, \quad t \geq T_0, \quad i,j = 1, \ldots, M$. The Definition 1 ensures that the multi-agent system (MAS) achieves practical consensus. □

Remark 4: From Remark 2, we know that an ideal controller v_i^d exists which can asymptotically stabilize the system $ds_i(t) = \left(\psi(s_i(t)) + v_i^d(t) + \hat{u}^a\right)dt + h_i(s_i(t))\, dW_i(t)$. However, since the nonlinear function $\psi(s_i)$ is unknown, the explicit form of $v_i^d(t)$ cannot be directly obtained. To address this, a neural network (NN)-based control approach is adopted to approximate the ideal controller. During system operation, the state $s_i(t)$ can be measured via sensors, enabling us to update the NN parameters online using the designed adaptation laws given in Eqs. (8) and (9). Specifically, the approximation capability of NNs is utilized to express the unknown controller in a generalized form. Although the NN parameters at the start are unknown, they may be estimated using the response from the system's measured positions. The NN adaptation laws are developed based on a Lyapunov function framework.

These laws are structured to ensure that the estimation error remains constant and decreases at event-triggering instants.

Remark 5: The condition $\psi(P,\Gamma) \subset M(H)$ in Theorem 1 may be verified by representing it as a linear matrix inequality format [43], which is identical to the condition

$$(L \otimes H)_i (I_N \otimes \frac{P}{\Gamma})^{-1} (L \otimes H)_i^T \leq 1, \tag{39}$$

where $(\cdot)_i$ shows the i-th row of the matrix.

Remark 6: The Eq. (17) to determine the next triggering moment, it just requires considering its position and the nearby states of the most [44] recent triggering moment. As mentioned, the communication load can be significantly decreased. Theorem 1 postulates the presence of a positive, nonzero lower bound in inert-event time.

Theorem 2: *Consider the nonlinear MAS described by Eq. (1), with control inputs given by Eqs. (2) and (7). Suppose that Assumptions 1–4 hold, and the neural network (NN) weights are modified according to Eqs. (8) and (9), even when the event-triggered condition in Eq. (17) is violated. Then, the inter-event time for the k-th triggering instant of agent i, defined as* $\delta\tau_k^i = \tau_{k+1}^i - \tau_k^i$, *is guaranteed to be lower bounded by a strictly positive constant for all* $k = 0, 1, \ldots,$ *and* $i = 1, 2, \ldots$

Proof: The Eq. (14), we can get the following inequality:

$$\|\dot{s}_i\| \leq \|A\|\|s_i\| + \gamma_{i,k}^1, \quad \tau_k^i \leq t < \tau_{k+1}^i, \tag{40}$$

where

$$\gamma_{i,k}^1 = \|\tilde{M}_{vi}\| q_{v,\max} + \varepsilon_{v,\max} + 2\|\hat{M}_{vi}\| q_{v,\max} + K_k^i \|e_i\|$$

is a function that remains constant over intervals.

Now, consider the error in estimation $\tilde{s}_i$. Its derivative satisfies:

$$\|\dot{\tilde{s}}_i\| = \|\dot{s}_i - \dot{\hat{s}}_i\| = \|\dot{s}_i\| \leq \|A\|\|s_i\| + \gamma_{i,k}^1, \quad \tau_k^i \leq t < \tau_{k+1}^i. \tag{41}$$

According to the comparison lemma, the solution of (41) subject to the initial condition $\tilde{s}_i(\tau_k^i) = 0$ is upper bounded by

$$\|\tilde{s}_i\| \leq \int_{\tau_k^{i+}}^{t} e^{\|A\|(t-s)} \gamma_{i,k}^1 ds = \frac{\gamma_{i,k}^1}{\|A\|} \left(e^{\|A\|(t-\tau_k^i)} - 1 \right), \quad \tau_k^i \leq t < \tau_{k+1}^i. \tag{42}$$

Furthermore, the inter-event time $\delta\tau_k^i = \tau_{k+1}^i - \tau_k^i$ corresponds to the time required for $\|\tilde{s}_i\|$ to grow from 0 to a predefined threshold:

$$\min_k \left(\frac{1}{Lq_v \|\hat{M}_{vi}\|} \left(\frac{q_{\min}\Gamma}{4\|P\|} \|s_i\| - K_k^i D_{max} \|e_i\| + \frac{\varsigma}{\|P\|} \right) \right) > 0$$

Substituting into the upper bound yields:

$$\delta\tau_k^i \geq \frac{1}{\|A\|} \ln \left(1 + \frac{\|A\| \min_k \left(\frac{1}{Lq_v \|\hat{W}_{vi}\|} \left(\frac{q_{\min}\Gamma}{4\|P\|} \|s_i\| - K_k^i D_{\max} \|e_i\| + \frac{\varsigma}{\|P\|} \right) \right)}{\gamma_{i,k}^1} \right)$$

$$\delta\tau_i^k > \frac{1}{\|A\|} \ln\left(1 + \frac{\|A\| \min_k \left(\frac{\varsigma}{Lq_v \|\hat{M}_{vi}\| \|P\|}\right)}{\gamma_{i,k}^1}\right) \tag{43}$$

Finally, as established in the proof of Theorem 1, both $\hat{M}_{vi}$ and e_i are bounded. Therefore, $\delta\tau_k^i$ is guaranteed to be greater than a strictly positive constant. □

4 Numerical Simulations

This section provides two numerical examples to illustrate how well the planned algorithm performs. The examples will demonstrate how well both Theorems 1 and 2 work.

Example 1: *The nonlinear MAS considered in this simulation operates over a directed communication topology depicted in Fig. 1, consisting of 5 agents labeled 1 to 5. The Laplacian matrix associated with this topology is:*

$$L = \begin{bmatrix} 1 & -1 & 0 & 0 & 0 \\ 0 & 2 & -1 & 0 & -1 \\ 0 & 0 & 1 & -1 & 0 \\ 0 & 0 & 0 & 1 & -1 \\ -1 & -1 & 0 & 0 & 1 \end{bmatrix}.$$

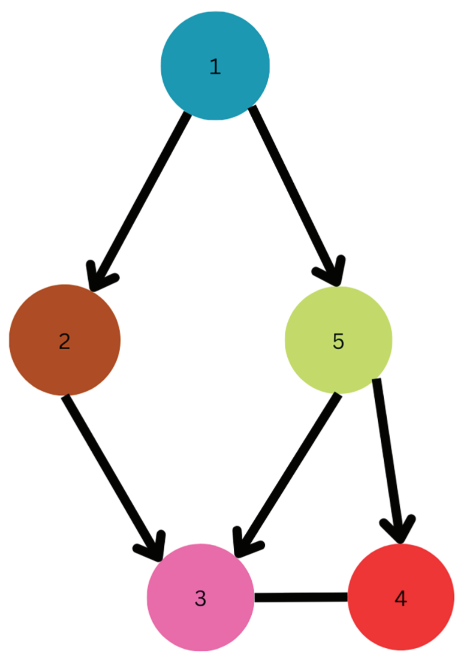

Figure 1: Communication topology

Each agent's dynamics are described by:

$$\begin{bmatrix} ds_{i1}(t) \\ ds_{i2}(t) \end{bmatrix} = \left(\begin{bmatrix} s_{i2}(t) \\ s_{i1}^3(t) - s_{i2}(t) \end{bmatrix} + u_i(t) + u_i^a(t)\right)dt + h_i\big(s_i(t)\big)\, dW_i(t) \tag{44}$$

where $u_i(t) = \left[\ u_{i1}, u_{i2}\ \right]$

The starting position of the five agents is given by:

$$s_1 = [5 - 11]^T, \quad s_2 = [13 - 12]^T, \quad s_3 = [11 - 13]^T, \quad s_4 = [8 - 10]^T, \quad s_5 = [7 - 8]^T.$$

The system matrix after feedback linearization is:

$$B = \begin{bmatrix} 0 & 1 \\ -3 & -4 \end{bmatrix}, \quad Q = \text{diag}\{0.1, 0.1\}.$$

From Theorem 1, the matrix P is derived as:

$$P = \begin{bmatrix} 60 & 1 \\ 1 & 60 \end{bmatrix}, \quad q_{\min} = 0.1.$$

We select design parameters as $\Gamma = 0.2$*,* $\varsigma = 0.09$*,* $\beta = 10^5$*, and* $H = diag\{0.006, 0.004\}$*. The disturbance matrices are:*

$$D_1 = \begin{bmatrix} 0.1 & 0 \\ 0 & 0.1 \end{bmatrix}, \quad D_2 = \begin{bmatrix} 0.5 & 0 \\ 0 & 0 \end{bmatrix}, \quad D_3 = \begin{bmatrix} 0.5 & 0 \\ 0 & 0.5 \end{bmatrix}, \quad D_4 = \begin{bmatrix} 0 & 0 \\ 0 & 0.2 \end{bmatrix},$$

with $D_{\max} = 1$*. The control gain* K_k^i *is computed via Eq. (17). The practical consensus bound is chosen as* $B_{\max}^s = 0.1$*.*

Each neural network has an Eq. (14) hidden layer neurons, with an input layer weight matrix $H_v \in \mathbb{R}^{2\times 15}$*, the elements are started from 0.5. The* $q(s_i)$ *is used in* $\tanh(H_v^T \hat{s}_i(t))$*, which has a Lipschitz constant* $L_{q_v} = \|H_v\| < 2.74$*. The neural network parameters are set as* $\alpha_v = 0.002$*,* $c = 1.5$*,* $\kappa = 0.002$*, and* $L = I.5$*. Initial weights of the Neural networks are* $\hat{M}_{vi}(0) = 0.005$*. A sampling time of 0.006 s is used. The gain* K_k^i *is selected randomly in the interval* $(0, 1)$*, scaled by the term*

$$\frac{q_{\min}\beta\|s_i\|}{4D_{\max}\|P\|\|e_i\|}.$$

The topology of directed communication between the five agents is shown in Fig. 1. The directed edges show the information flow between each node, which stands for an agent. While Agent 2 speaks with Agent 3, Agent 1 provides information to Agents 2 and 5. In a similar manner, Agent 5 sends information to Agents 3 and 4, and Agent 4 then forwards that information to Agent 3. Under the suggested control scheme, this structure makes sure that the network is connected and that information can spread among all agents, which makes reaching consensus easier.

The evolution of the agents' first-state components is illustrated in the top plot in Fig. 2, where $s_1(t)$ *is shown along the x- and y-axes. Each agent begins from a distinct initial position and exhibits brief oscillatory behavior before converging to a common consensus trajectory. The states gradually decay toward zero, indicating consistent and well-coordinated behavior under the proposed control law. The corresponding control inputs* $u_1(t)$ *in the x- and y-directions are presented in the bottom plot. Initially, the control effort increases to compensate for the state deviations, followed by a smooth reduction as the agents achieve coordination. Both control components remain bounded and eventually settle within a small neighborhood around zero once consensus is reached. These results confirm that the agents' motion is effectively regulated and verify the stability of the designed control strategy.*

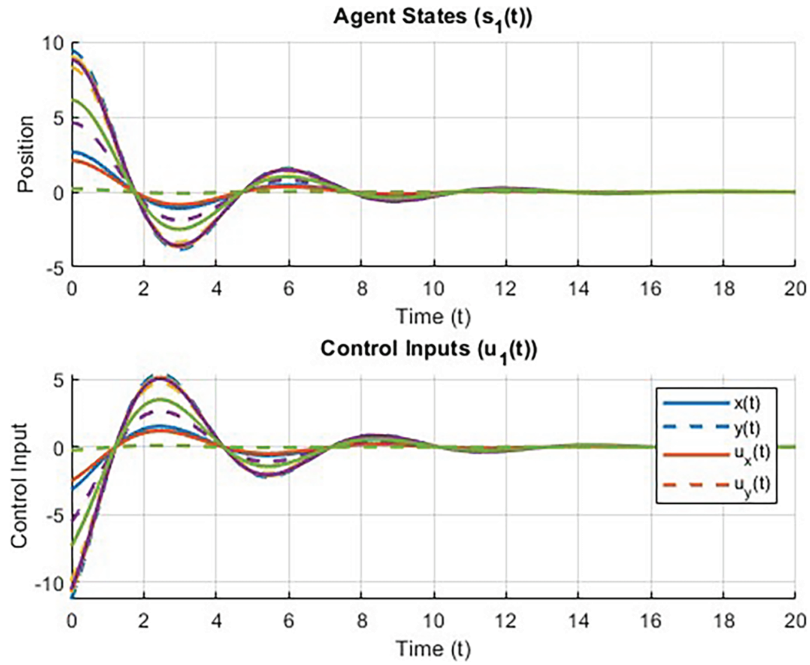

Figure 2: Agent state and Control input

Fig. 3 illustrates the evolution of the neural network (NN) weight norms together with the corresponding agent state trajectories. The upper subplot shows the NN weight–norm convergence surface for all agents, where the vertical axis represents the magnitude $\|M_i(t)\|$ and the surface demonstrates that all weight estimates decay smoothly over time, indicating successful adaptation and parameter convergence. The lower subplot depicts the state trajectories $x_i(t)$ and $y_i(t)$ for all agents. Despite initial differences and transient oscillations, the states of all agents converge asymptotically toward the desired equilibrium. The combination of the two plots highlights that the adaptive control law not only stabilizes the multi-agent system but also ensures bounded and convergent NN weight estimates.

Example 2: *For a class of heterogeneous multi-agent systems (MAS) fulfilling Assumption 2. Suppose that a MAS consisting of the given five subsystems with different nonlinear dynamics:*

$$\begin{aligned}
\begin{bmatrix} ds_{11}(t) \\ ds_{12}(t) \end{bmatrix} &= \left(\begin{bmatrix} s_{12}(t) \\ s_{11}^3(t) - s_{12}(t) \end{bmatrix} + u_i(t) + u_i^a(t) \right) dt + h_i(s_i(t))\, dW_i(t) \\
\begin{bmatrix} ds_{21}(t) \\ ds_{22}(t) \end{bmatrix} &= \left(\begin{bmatrix} s_{22}(t) \\ s_{21}^3(t) - s_{22}(t) \end{bmatrix} + u_i(t) + u_i^a(t) \right) dt + h_i(s_i(t))\, dW_i(t) \\
\begin{bmatrix} ds_{31}(t) \\ ds_{32}(t) \end{bmatrix} &= \left(\begin{bmatrix} s_{32}(t) \\ s_{31}^3(t) - s_{32}(t) \end{bmatrix} + u_i(t) + u_i^a(t) \right) dt + h_i(s_i(t))\, dW_i(t) \\
\begin{bmatrix} ds_{41}(t) \\ ds_{42}(t) \end{bmatrix} &= \left(\begin{bmatrix} s_{42}(t) \\ s_{41}^3(t) - s_{42}(t) \end{bmatrix} + u_i(t) + u_i^a(t) \right) dt + h_i(s_i(t))\, dW_i(t) \\
\begin{bmatrix} ds_{51}(t) \\ ds_{52}(t) \end{bmatrix} &= \left(\begin{bmatrix} s_{52}(t) \\ s_{51}^3(t) - s_{52}(t) \end{bmatrix} + u_i(t) + u_i^a(t) \right) dt + h_i(s_i(t))\, dW_i(t)
\end{aligned} \tag{45}$$

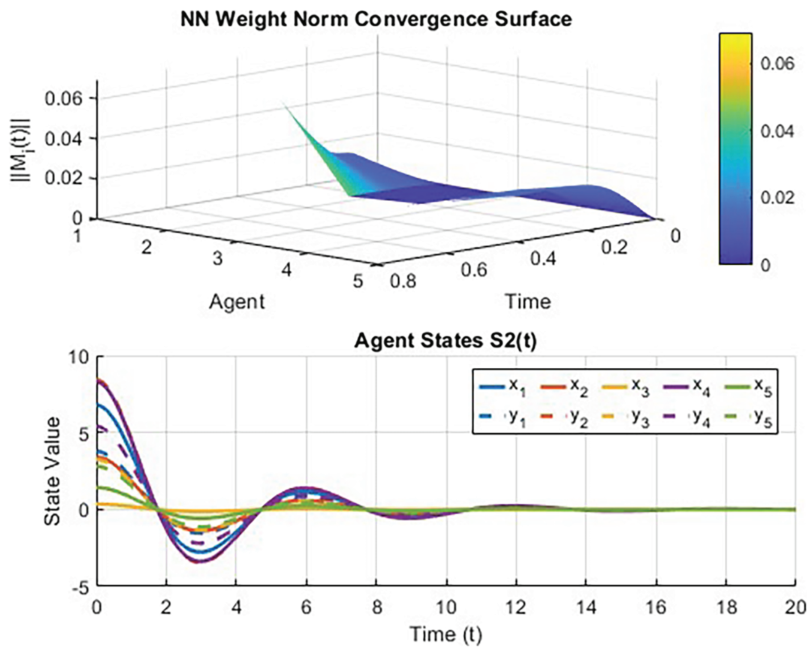

Figure 3: Weight norm convergence

The control input and weight convergence surfaces in Fig. 4 together provide strong evidence of the closed-loop system's stability. In the control input surface, the transient oscillations observed at the beginning gradually diminish as time progresses, and the control efforts converge toward small steady-state values. This reduction in control magnitude indicates that the tracking errors are effectively driven to zero, and the system no longer requires significant corrective action—a key property of asymptotic stability. Complementing this, the weight convergence surface shows that the adaptive neural network weights evolve smoothly and remain bounded throughout the operation. After an initial period of adaptation, the weight norms settle into a steady trend without exhibiting divergence or instability. This bounded and convergent weight behavior confirms that the adaptive learning mechanism does not destabilize the system. Together, these two surfaces demonstrate that the proposed controller ensures stable closed-loop performance, guaranteeing that both the agent states and adaptive parameters converge in a well-behaved and stable manner.

Fig. 5 illustrates the comparison of agent state trajectories obtained using the baseline consensus method and the proposed control strategy. The dashed curves represent the baseline approach, while the solid curves correspond to the proposed method. It can be observed that, although both methods eventually achieve consensus, the proposed approach exhibits a significantly faster convergence rate. Specifically, the agent states under the proposed controller rapidly converge to a common equilibrium value with reduced oscillations, whereas the baseline method shows slower convergence and larger transient deviations. These results clearly demonstrate the superior convergence performance of the proposed method, highlighting its effectiveness in improving consensus speed while maintaining system stability.

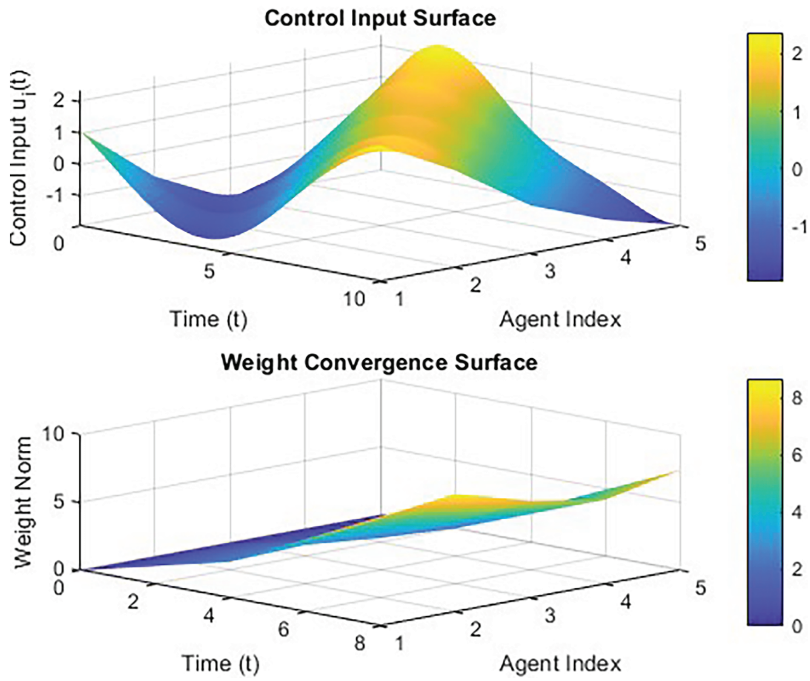

Figure 4: Control input and Weight convergence

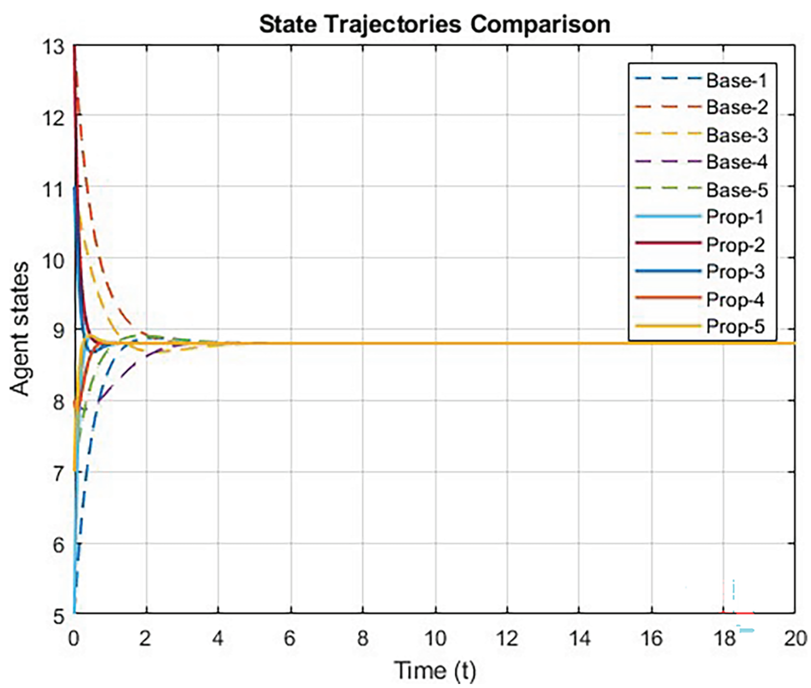

Figure 5: State trajectories comparison

5 Conclusion

In this work, an adaptive self-triggered consensus control based on neural networks was proposed for nonlinear multi-agent systems that are concerned with cyber-physical attacks, stochastic disturbances, and sensor saturation. In addition to avoiding Zeno behavior and ensuring practical consensus, the scheme minimizes communication overhead and remains resilient to adversarial attacks and uncertainties. It is a safe, effective, and scalable solution for actual networked control applications, as demonstrated by simulation results on both homogeneous and heterogeneous systems. All things considered, the framework provides networked multi-agent systems functioning in unpredictable and hostile environments with a scalable, secure, and energy-efficient consensus solution.

Acknowledgement: This work has been carried out at Huainan Normal University and at University of Lahore, Sargodha Campus. The authors are also grateful for the support from Northern Border University, Al Ahliyya Amman University Amman, Jordan and King Khalid University Saudi Arabia.

Funding Statement: This article is supported by the National Natural Science Foundation of China (12301185), the Natural Science Foundation of Higher Education Institutions in Jiangsu Province under Grant 22KJB110013, the natural science research foundation of colleges and universities of Anhui Province (2024AH051719) and The authors also express their appreciation to the Deanship of Scientific Research at Northern Border University, Arar, Saudi Arabia for funding this research work through project number NBU-FFR-2025-2920-09.

Author Contributions: The authors confirm contribution to the paper as follows: Conceptualization, Jun Du; Software, Naveed Iqbal; Validation, Hanen Louati; Formal analysis, Azmat Ullah Khan Niazi; Resources, M. M. A. Almazah; Writing-original draft, Muhammad Zahid, Jun Du; Writing-review & editing, Muhammad Zahid, Jun Du; Supervision, Azmat Ullah Khan Niazi; Project administration, Jun Du, Hanen Louati. All authors reviewed the results and approved the final version of the manuscript.

Availability of Data and Materials: Data sharing not applicable to this article as no datasets were generated or analysed during the current study. The code is considered an intellectual property of University of Lahore, Sargodha Campus, Pakistan, and therefore not publicly available.

Ethics Approval: Not applicable.

Conflicts of Interest: The authors declare no conflicts of interest to report regarding the present study.

References

1. Li Z, Hu J, Leng B, Xiong L, Fu Z. An integrated of decision making and motion planning framework for enhanced oscillation-free capability. IEEE Trans Intell Transp Syst. 2023;25(6):5718–32. doi:10.1109/TITS.2023.3332655.
2. Ju X, Jiang Y, Jing L, Liu P. Quantized predefined-time control for heavy-lift launch vehicles under actuator faults and rate gyro malfunctions. ISA Trans. 2023;138:133–50. doi:10.1016/j.isatra.2023.02.022.
3. Hu J, Chen B, Ghosh BK. Formation-circumnavigation switching control of multiple ODIN systems via finite-time intermittent control strategies. IEEE Trans Control Netw Syst. 2024;11(4):1986–97. doi:10.1109/TCNS.2024.3371597.
4. Yu L, Wu L. Towards byzantine-resilient federated learning via group-wise robust aggregation. In: Federated learning: privacy and incentive. Cham, Switzerland: Springer International Publishing; 2020. p. 81–92.

5. Chen J, Li M, Marcantoni M, Jayawardhana B, Wang Y. Range-only distributed safety-critical formation control based on contracting bearing estimators and control barrier functions. IEEE Internet Things J. 2025;12(19):40968–79. doi:10.1109/JIOT.2025.3590774.
6. Xu G, Lei L, Mao Y, Li Z, Chen XB, Zhang K. CBRFL: a framework for committee-based Byzantine-resilient federated learning. J Netw Comput Appl. 2025;238:104165. doi:10.1016/j.jnca.2025.104165.
7. Zhang K, Wang H, Chen M, Chen X, Liu L, Geng Q, et al. Leveraging machine learning to proactively identify phishing campaigns before they strike. J Big Data. 2025;12(1):124. doi:10.1186/s40537-025-01174-x.
8. Liu J, Jiang G, Chu C, Li Y, Wang Z, Hu S. A formal model for multiagent Q-learning on graphs. Sci China Inf Sci. 2025;68(9):192206. doi:10.1007/s11432-024-4289-6.
9. Xiong JJ, Wang XY, Li C. Recurrent neural network based sliding mode control for an uncertain tilting quadrotor UAV. Int J Robust Nonlinear Control. 2025;35(18):8030–46. doi:10.1002/rnc.70108.
10. Xie WT, Song DN, Tang WC, Ma JW, Li JH. Auxiliary support path planning for robot-assisted machining of thin-walled parts with non-uniform thickness and closed cross-section based on a neutral surface. J Manuf Process. 2025;147:16–28. doi:10.1016/j.jmapro.2025.05.002.
11. Liu X, Wu C, Zhen S, Sun H, Sun C, Chen YH. Robust control under servo constraint following via nash equilibrium theory for bimanual humanoid manipulation. IEEE Trans Fuzzy Syst. 2025;33(11):4069–82. doi:10.1109/TFUZZ.2025.3609828.
12. Zhou L, Li Z, Li Y, Bai S. Parallel MPPI with gradient-velocity modulated SDF cost for high-performance real-time dynamic obstacle avoidance by robot manipulators. IEEE Trans Robot. 2025;41:5149–68. doi:10.1109/TRO.2025.3600125.
13. Lu Q, Wu X, She J, Guo F, Yu L. Disturbance rejection for systems with uncertainties based on fixed-time equivalent-input-disturbance approach. IEEE/CAA J Automat Sinica. 2024;11(12):2384–95. doi:10.1109/JAS.2024.124650.
14. Montenbruck JM, Bürger M, Allgöwer F. Practical synchronization with diffusive couplings. Automatica. 2015;53:235–43. doi:10.1016/j.automatica.2014.12.024.
15. Li H, Liu Q, Feng G, Zhang X. Leader-follower consensus of nonlinear time-delay multiagent systems: a time-varying gain approach. Automatica. 2021;126:109444. doi:10.1016/j.automatica.2020.109444.
16. Zhao J, Lv Y, Zhao Z, Wang Z. Adaptive optimal tracking control of servo mechanisms via generalised policy learning. IEEE Trans Instrum Meas. 2024;73:3002311. doi:10.1109/TIM.2024.3457963.
17. Zhang K, Wang Y, Bhatti UA, Zhou Y, Jin M. Enhanced ransomware attacks detection using feature selection, sensitivity analysis, and optimized hybrid model. J Big Data. 2025;12(1):245. doi:10.1186/s40537-025-01289-1.
18. Ding F, Liu Z, Wang Y, Liu J, Wei C, Nguyen AT, et al. Intelligent event triggered lane keeping security control for autonomous vehicle under DoS attacks. IEEE Trans Fuzzy Syst. 2025;33(10):3595–608. doi:10.1109/TFUZZ.2025.3597276.
19. Zhu H, Liu J, Zhang S, Zhang Z, Qu F. HDWM-based consensus control for multi-agent systems under communication delays and DoS attacks. Int J Cont Automat Syst. 2023;21(12):3896–908. doi:10.1007/s12555-022-0609-3.
20. Yuan W, Chen J, Chen S, Feng D, Hu Z, Li P, et al. Transformer in reinforcement learning for decision-making: a survey. Front Inform Technol Elect Eng. 2024;25(6):763–90. doi:10.1631/FITEE.2300548.
21. Raza MH, Rehan M, Ali PR, Hong KS. Bipartite consensus of heterogeneous multi-agents under input saturation over signed graphs. IEEE Trans Circ Syst II: Exp Briefs. 2023;70(9):3398–402. doi:10.1109/TCSII.2023.3258751.
22. He W, Tan J, Wang R, Liu Z, Luo X, Hu H, et al. A deep reinforcement learning approach to time delay differential game deception resource deployment. IEEE Trans Dependable Secure Comput. 2025. doi: doi:10.1109/TDSC.2025.3620151.

23. Li YY, Li YX. Resilient distributed fixed-time tracking of heterogeneous UAV-UGV systems against DoS attacks. IEEE Trans Syst Man Cybernet: Syst. 2024;54(9):5780–90. doi:10.1109/TSMC.2024.3408410.
24. Fu Y, Wang B, Zhao H, Zhou M, Li N, Gao Z. Adaptive safety attitude control of a hybrid VTOL UAV under transition flight subject to multiple faults and uncertainties. Aerosp Sci Technol. 2025;163:110284. doi:10.1016/j.ast.2025.110284.
25. Wu Z, Zhang H. Review on autonomous and sustainable urban mobility systems: challenges and future directions. Authorea Preprints. 2025 [cited 2025 Dec 2]. Available from: https://www.techrxiv.org/users/692350/articles/1335052-review-on-autonomous-and-sustainable-urban-mobility-systems-challenges-and-future-directions.
26. Xu G, Fan X, Xu S, Cao Y, Zhang K, Kang J, et al. Towards authenticated encrypted search with constant trapdoor for mobile cloud systems. IEEE Trans Mobile Comput. 2025. doi:10.1109/TMC.2025.3627241.
27. Chen P, Song Y, Xia Y. Adaptively diagnosing system faults in microservice architecture: an autonomous predictive model construction framework. Future Gener Comput Syst. 2025;177:108256. doi:10.1016/j.future.2025.108256.
28. Jiang X, Xia G, Feng Z, Han QL, Su R. On estimation of reachable sets for approximate consensus of homogeneous multiagent systems subject to bounded exogenous disturbances. IEEE Trans Netw Sci Eng. 2023;10(6):3184–97. doi:10.1109/TNSE.2023.3252598.
29. Zhang B, Xue Y, Zhang Y, Su K. A self-calibrating digital twin for space thermionic nuclear reactors under fault conditions. Reliab Eng Syst Safety. 2025;268:111995. doi:10.1016/j.ress.2025.111995.
30. Song DN, Tang WC, Zhao YN, Zhong YG, Ma JW. Convolution-based velocity-smoothing principle and its application to real-time parametric curve interpolation. IEEE Trans Autom Sci Eng. 2025;22:23443–54.
31. Das S, Tesfamariam S. Reliability assessment of stochastic dynamical systems using physics-informed neural network-based PDEM. Reliab Eng Syst Safety. 2024;243:109849. doi:10.1016/j.ress.2023.109849.
32. Li B, Wang P, Shao Z, Liu A, Jiang Y, Li Y. Defending Byzantine attacks in ensemble federated learning: a reputation-based phishing approach. Future Gener Comput Syst. 2023;147:136–48. doi:10.1016/j.future.2023.05.002.
33. Wang W, Li Y, Tong S. Neural-network-based adaptive event-triggered consensus control of nonstrict-feedback nonlinear systems. IEEE Trans Neural Netw Learn Syst. 2020;32(4):1750–64. doi:10.1109/TNNLS.2020.2991015.
34. Zhou Z, Abawajy J, Chowdhury M, Hu Z, Li K, Li F, et al. Minimizing SLA violation and power consumption in Cloud data centers using adaptive energy-aware algorithms. Future Gener Comput Syst. 2018;86:836–50. doi:10.1016/j.future.2017.07.048.
35. Zhou Z, Shojafar M, Alazab M, Abawajy J, Li F. AFED-EF: an energy-efficient VM allocation algorithm for IoT applications in a cloud data center. IEEE Trans Green Commun Netw. 2021;5(2):658–69. doi:10.1109/TGCN.2021.3067309.
36. Jiang C, Du H, Zhu W, Yin L, Jin X, Wen G. Synchronization of nonlinear networked agents under event-triggered control. Inf Sci. 2018;459:317–26. doi:10.1016/j.ins.2018.04.058.
37. Hu T, Lin Z. Control systems with actuator saturation: analysis and design. Cham, Switzerland: Springer Science & Business Media; 2001.
38. Khalil HK, Grizzle JW. Nonlinear systems. Vol. 3. Upper Saddle River, NJ, USA: Prentice Hall; 2002.
39. Li H, Chen G, Huang T, Zhu W, Xiao L. Event-triggered consensus in nonlinear multi-agent systems with nonlinear dynamics and directed network topology. Neurocomputing. 2016;185:105–12. doi:10.1016/j.neucom.2015.12.047.
40. Zhong M, Zhang J, Zheng G, Liu H. Data-driven model-free adaptive dynamic programming resilient control for nonlinear networked control systems under DoS attacks. IEEE Trans Cybern. 2025;55(12):5700–13. doi:10.1109/TCYB.2025.3594793.

41. Yang X, Zhang X, Cao J, Liu H. Observer-based adaptive fuzzy fractional backstepping consensus control of uncertain multiagent systems via event-triggered scheme. IEEE Trans Fuzzy Syst. 2024;32(7):3953–67. doi:10.1109/TFUZZ.2024.3386312.
42. Haddad WM, Chellaboina V, Nersesov SG. Impulsive and hybrid dynamical systems: stability, dissipativity, and control. Princeton, NJ, USA: Princeton University Press; 2016.
43. Zhang T, Zhang H, Xie X. Region stability/stabilization and H_∞ control for discrete-time impulsive Takagi–Sugeno fuzzy systems. IEEE Trans Fuzzy Syst. 2024;32(6):3410–9.
44. Zheng S, Shi P, Wang S, Shi Y. Event triggered adaptive fuzzy consensus for interconnected switched multiagent systems. IEEE Trans Fuzzy Syst. 2019;27:144–58. doi:10.1109/TFUZZ.2018.2873968.